

A Forward Solution for RF Impedance Tomography in Wood

¹Ian WOODHEAD, ²Nobuo SOBUE, ¹Ian PLATT, ³John CHRISTIE

¹Lincoln Technology

Lincoln Ventures Ltd, Lincoln University, New Zealand

²Faculty of Agriculture

Shizuoka University, Shizuoka, 422-8529, Japan

³Streat Technology Ltd.

c/o Lincoln Ventures Ltd, Lincoln University, New Zealand,

E-mail: woodhead@lvl.co.nz, sobue@shizuoka.ac.jp, platti@lvl.co.nz, christij@lvl.co.nz

Received: 15 October 2007 / Accepted: 20 February 2008 / Published: 15 April 2008

Abstract: Both integral equation and differential equation methods enable modelling current and hence impedance of wood, to provide the forward solution for impedance tomography that in turn provides a measure of its internal moisture distribution. Previously, we have used a series impedance model and successfully demonstrated measurement of internal moisture distribution. Here we describe the adaptation of our integral equation method for this application. This has required an alternative calculation to model the impressed field from the segmented electrodes used in the measurements to date, and we demonstrate distortion of the anomalous field due to the presence of a wood dielectric, and the field magnitude. Further work will be required to translate the resulting field distribution from our model, to complex current and hence impedance readings, to allow completion of tomographic reconstruction using this approach. *Copyright © 2008 IFSA.*

Keywords: Impedance, Tomography, Heterogeneous, Model, Wood

1. Introduction

Water has several distinctive properties that may be used for measurement of moisture content in composite materials. One is that the bond angle of 104.47 degrees [1] between the hydrogen atoms, combines with the differing electronegativity of the hydrogen (2.1) and oxygen (3.5) atoms to result in a large polar moment. The strong polar nature of the water molecule contributes to the large relative permittivity (ϵ_r) of approximately 80 for bulk water compared to that of most dry biological and

natural materials for which ε_r is generally in the range 2 to 5 [2]. This large contrast enables dielectric measurements of composite materials to form a useful indirect measurement of volumetric moisture content (θ_v). In practice, ε_r is a curvilinear function of θ_v , whose curvature is dependent on the composite material, its texture, and its porosity which influence the interaction of the composite material with water.

ε_r arises primarily from polar molecules that store energy by elastic rotation, but contributions are also made by elastically altering bond angles, and intra-atomic contributions that are dominated by distortion of electron distribution. In the absence of an electric field, a polar substance such as water has permanent dipole moments that are randomly distributed so that no net polarization is present. The conductivity of the material and any conducting inclusions (e.g. dissociated water) dispersed within the material contribute to the dielectric loss of the mixture. The total permittivity ε comprises a real component ε' that represents the real or energy storage component of the permittivity, and ε'' the orthogonal or imaginary component that results from the conduction current contributed to by conductivity and other forms of dielectric loss.

$$\varepsilon = \varepsilon' - j\varepsilon'', \quad (1)$$

where j is $\sqrt{-1}$. Many methods of determining ε' are usefully employed for determining θ_v of composite materials. However where ε'' is large in comparison with ε' , the measurement becomes inaccurate [3]. Consequently, the choice of measurement frequency range when measuring ε' is crucial since many loss processes are frequency dependent.

For measurement of moisture content in wood, both ε' and ε'' have been explored such as described by [4], and provided the frequency is chosen to avoid the dispersive low frequency regions either or both measures may be used to provide a useful indication of moisture content.

We [5] have demonstrated the utility of applying impedance tomography to measurement of the internal moisture distribution in wood (Fig. 1), and using time domain reflectometry techniques [6]. Here we apply the electromagnetic model of [7] to the impedance tomography problem described by [5].

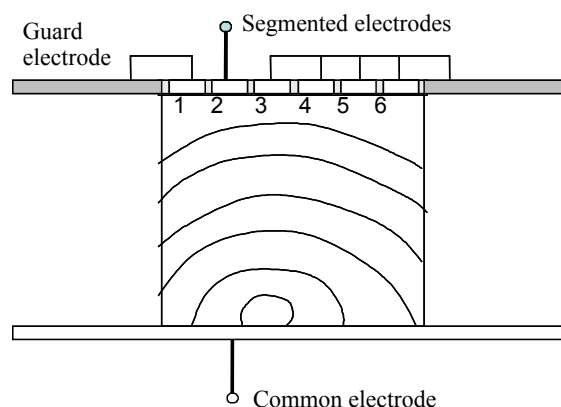


Fig. 1. Configuration of the segmented electrodes for measurement of the internal moisture distribution in wood described by Sobue and Inagaki (2007).

There are two main advantages of an integral equation model for this type of problem. The first is that since only the anomalous region (that occupied by the wood) needs to be modelled, the domain of the

problem need only include the timber cross-section and the segmented electrodes or capacitor plates (Fig. 1); the region beyond makes no contribution. Using a differential equation model, requires setting external boundary conditions, which may include the electrodes, but for accurate modelling needs to extend well beyond the region of the wood to where the field may be assumed to be zero. The second advantage of an integral equation approach is that the problem may be solved once for a given moisture distribution and for any field distribution representing different segments of the electrodes, resulting in just one forward calculation per inverse iteration. Again this contrasts with differential equation methods where one solution would be required for each capacitor electrode configuration. The approach is thus generally more favourable for inverting measurements than the otherwise more rapid differential equation methods.

We first provide some background to the integral equation approach, and then explain how we configured the impressed or incident field for application to this problem and show results from that simulation. Finally we describe the remaining work to complete the solution.

2. Theory

The polarization of a discretized zone or cell within a dielectric material may be represented by a dipole at its geometric centre. In most dielectric materials, there is no net polarization until generated by an external or impressed field. When applied to this quasi-static electric field problem where the material is considered lossless, the method of moments may be considered as the summation in each cell of the electric field contributions due to the polarization in all other cells. Using rectangular coordinates, the potential ϕ_p at point $p(x, y, z)$ generated by polarization P , is:

$$\phi_p = \frac{\tilde{P} \cdot \hat{r}}{4\pi\epsilon_0 r^2}, \quad (2)$$

where \hat{r} is a unit vector pointing from the centre of the cell to p [8], and r is the distance from the cell centre to p . In Cartesian 3-space:

$$\phi_p = \frac{\tilde{P} \cdot (\tilde{x}, \tilde{y}, \tilde{z})}{4\pi\epsilon_0 r^3}, \quad (3)$$

where \tilde{x}, \tilde{y} and \tilde{z} are the rectangular components of \tilde{r} . The potential arising from the contribution from many cells is:

$$\phi_p = \iiint \frac{\tilde{P} \cdot \hat{r}}{4\pi\epsilon_0 r^2} dv, \quad (4)$$

where dv is the differential volume over which each $P \cdot \hat{r}$ applies. Reverting to the single dipole case, its electric field is the space rate of change of potential ($-\nabla\phi_p$) so that from equation 3:

$$E_{px} = \frac{-\tilde{P}}{4\pi\epsilon_0 r^5} \cdot \left[\hat{x}(r^2 - 3x^2) - \hat{y}(3xy) - \hat{z}(3xz) \right] \quad (5)$$

with corresponding equations for E_{py} and E_{pz} . The above may be combined in an integral equation describing the electric field E_p at a point p :

$$\mathbf{E}_p(x, y, z) = -\nabla \left(\iiint \frac{\mathbf{P} \cdot \mathbf{r}}{4\pi\epsilon_0 r^2} dv \right) \quad (6)$$

The polarization region may now be discretized, and following the method of moments [9], we calculate the matrix of polarization vectors $P(x, y, z)$ using:

$$\begin{aligned} L(\mathbf{P}) &= -\mathbf{E}_i(x, y, z) \\ &= \mathbf{E}_p(x, y, z) - \frac{\mathbf{P}(x, y, z)}{\epsilon_0 \chi(x, y, z)}, \end{aligned} \quad (7)$$

where L is a linear operator, E_i the external impressed field and $\chi(x, y, z)$ the electric susceptibility ($\epsilon_r(x, y, z) - 1$). Equation 7 is converted to matrix form and solved for the vector of polarizations P , and the electric field strength in each cell is recovered from the polarization:

$$\mathbf{E}(x, y, z) = \frac{\mathbf{P}(x, y, z)}{\epsilon_0 \chi(x, y, z)} \quad (8)$$

The model used here employs the pseudo 3-D method [7] which effectively reduces the problem to 2-D, and uses field proximity compensation as described in [6] to obtain improved prediction of the electric field distribution.

The inputs required to solve the forward solution are:

1. A vector describing the impressed field
2. A matrix describing the complex permittivity within each cell
3. Details of the dimensionality of the problem.

While the above method applies to any impressed field distribution, in this case E_i is the vector of impressed field components arising from two planar electrodes as in Fig. 1.

3. Modelling Planar Electrodes

To calculate the field from two planar electrodes, and continuing to use rectangular coordinates, we first define a small element of the planar electrode Δx , with a line charge density ρ and calculate the potential at a point p positioned a distance $r = \sqrt{x^2 + y^2}$ from the electrode element [8]. From electrostatic theory, e.g. [8], the x -component of the potential is defined as:

$$\phi_x = \frac{\rho \Delta x}{4\pi\epsilon_0 \sqrt{x^2 + y^2}} \quad (9)$$

Since the electric field E is the gradient of the potential, i.e. $\mathbf{E} = -\nabla\phi$, and using (9) to define the potential in the x and y directions, it can be shown that the two rectangular components of the field at p may be expressed as:

$$\begin{aligned} E_x &= \frac{\rho}{4\pi\epsilon_0} \int \left((x^2 + y^2)^{-\frac{1}{2}} - x(x^2 + y^2)^{-\frac{3}{2}} \right) dx \\ E_y &= \frac{\rho}{4\pi\epsilon_0} \int -y(x^2 + y^2)^{-\frac{3}{2}} dy \end{aligned} \quad (10)$$

The integrals are taken over the surfaces of both electrodes with appropriate consideration to the sign of ρ . Then applying the theory described in Section 2, the resultant electric field may be generated. Fig. 2 shows the incident or impressed electric field, when no wood is inserted between the electrodes, when using equations 10 to provide a vector of impressed field values in the model.

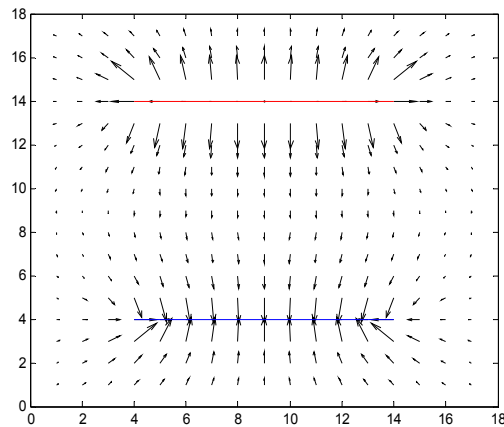


Fig. 2. Cross-sectional view (as in Fig. 1) showing the incident electric field distribution from two planar electrodes in air.

A typical result is shown in Fig. 3. In this case it arises from the forward solution applied to the region where a block of wood, $\epsilon_r = 3 + j3$, is positioned in the upper left region between the planar electrodes. It demonstrates the reduced field intensity within the wood compared with air, and the distortion of the surrounding field compared with Fig. 2. Note that in this instance, the electrodes have been defined as zero thickness, so there is an anomalous impact on the field outside the electrodes. The simplification has no effect on the field between the electrodes, with or without an included dielectric.

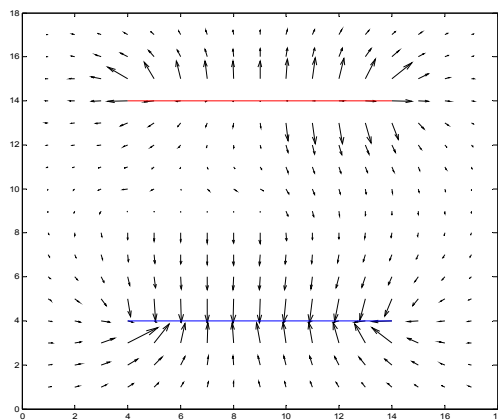


Fig. 3. Cross-sectional view (as in Fig. 2) showing the predicted electric field distribution when a block of wood is placed in the upper left region between the two planar electrodes.

4. Validation

We chose to validate the model by modelling the displacement current and hence predicting the capacitance of two planar electrodes with a PVC dielectric. A PVC block with $\epsilon_r = 3 + j0$ and with dimensions 50 by 50 by 148 mm was fitted with two self-adhesive foil electrodes of dimension 50 by

148 mm to form a capacitor. The measured capacitance, due to that of the capacitor itself plus the free-space capacitance of one plate at 250 kHz was 18.39 pF, so that the expected current from a 1V RMS source was 14.75 μ A.

The above model with a permittivity between the electrodes of $\epsilon_r = 3 + j0$, was used to calculate the electric field distribution for a potential difference between the electrodes of 1V RMS at 250 kHz. The displacement current density J_D , defined as dD/dt where D is electric displacement [11], can be written:

$$J_D = (1 + \chi)\epsilon_0 \frac{dE}{dt} \quad (11)$$

and hence the current is defined as:

$$i_D = (1 + \chi)\epsilon_0 l^2 \frac{dE}{dt} \quad (12)$$

where l is the edge length of the cubic cells. dE/dt for each cell was taken as the RMS value of the maximum dE/dt at 250 kHz, ωE . Since the forward solution represents the electrodes as sheet charge sources rather than conductors, the field and hence current outside the electrodes is affected by the dielectric between the electrodes. Hence the simulated displacement current has been taken as the sum of the total current with $\epsilon_r = 1 + j0$ and the difference between the current integrated along the inner face of the electrodes for the conditions $\epsilon_r = 3 + j0$ and $\epsilon_r = 1 + j0$. This provided a value of 15.14 μ A, compared with the 14.75 μ A value derived from measurements.

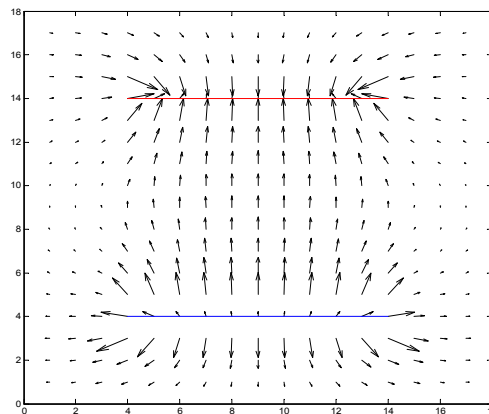


Fig. 4. Predicted displacement current for PVC dielectric between two planar electrodes.

5. Measurements in Wood

The validated forward solution described above is the major remaining step in providing a new impedance tomography method for measurement of moisture distribution in wood. The method of [5], configured according to Fig. 1, employed an instrument to measure the real and imaginary components of the impedance at 250 kHz. For an iterative inversion procedure to predict moisture distribution, the forward solution will need to be configured to predict the impedance between combinations of electrode segments which would then be compared with the measured values.

We explained above how an integral equation method conveys advantages for inverse methods, since little computational effort is required to provide a solution for each different configuration of the impressed field. In the method described by [5], guard electrodes were used, and hence we may make the approximation that the gaps between the electrode segments are arbitrarily narrow. In this case then, the electric field and current distribution remain constant, irrespective of which electrode segment is being measured, so that one forward calculation will suffice for each estimate of the wood impedance distribution in the inverse solution.

A further feature of this approach is that there is little computational overhead in providing values of impedance for many different measurement frequencies, and use of multiple frequencies is commonly used to extract a measure of product density. Hence we are keen to extend this work in the future to measurement of density distribution.

6. Conclusions

We have described a forward solution for calculating the impedance distribution in wood from its dielectric properties, and shown simulations of the electric field distribution in wood from the field of two parallel electrodes. The computational efficiency of the integral equation model has also been described and we forecast that this will have important industrial benefits. We have also predicted the displacement current in a PVC dielectric and provided good agreement with the measured value at 250 kHz. The next stage, is to apply the method to our earlier work which used a series model of impedance to provide tomographic reconstruction of the moisture distribution in wood.

Acknowledgement

This work was supported by the New Zealand Foundation for Research Science and Technology.

References

- [1]. F. Franks, Water, a comprehensive treatise, Vol. 1. The physics and physical chemistry of water, Ed. by J. B. Hasted, *Plenum Press*, London, 1972.
- [2]. S. O. Nelson, Electrical properties of agricultural products, a critical review, ASAE special publication SP-05-73, St Joseph, MI-ASAE, 1973.
- [3]. W. Leschnik and U. Schlemm, Measurement of the moisture and salt content of building materials, *3rd Workshop on Electromagnetic Wave Interaction with Water and Moist Substances*, USDA, Athens, Georgia, 1999.
- [4]. G. I. Torgovnikov, Dielectric properties of wood and wood-based materials, Ed. by T. E. Timel, *Springer Verlag*, Berlin, 1993.
- [5]. N. Sobue and M. Inagaki, *7th Conference on Electromagnetic Wave Interaction with Water and Moist Substances*, Hamamatsu, Japan, 2007.
- [6]. I. M. Woodhead, P. Riding, J. H. Christie and G. D. Buchan, Non-Invasive Measurement of Moisture Distribution, *Proceedings of the 2004 New Zealand National Conference on Non Destructive Testing*, Massey University, NZ, 2004.
- [7]. I. M. Woodhead, G. D. Buchan and D. Kulasiri. Pseudo-3-D Moment method for rapid calculation of electric field distribution in a low-loss inhomogeneous dielectric, *IEEE Transactions on Antennas and Propagation*, 49, 8, 2001, pp. 1117-1122.
- [8]. A. F. Kip, Fundamentals of Electricity and Magnetism, *McGraw-Hill*, 1962.
- [9]. R. F. Harrington, Field Computation by Moment Methods, *R E Kreiger*, 1968.

- [10].I. M. Woodhead, G. D. Buchan, I. G. Platt and J. H. Christie, Enhanced Integral Equation Modelling for Moisture Sensors, Sixth Conference on Electromagnetic Wave Interaction with Water and Moist Substances, *Weimar*, Germany, 2005, pp. 132-139.
 - [11].S. Ramo, J. R. Whinnery, and T. Van Duzer, *Fields and Waves in Communication Electronics*, Wiley, 1993.
 - [12].I. M. Woodhead, G. D. Buchan, I. G. Platt and J. H. Christie, *7th Conference on Electromagnetic Wave Interaction with Water and Moist Substances*, Hamamatsu, Japan, 2007.
-